DIFFUSION CHARACTERISTICS OF AIRBORNE PARTICLES WITH GRAVITATIONAL SETTLING IN A CONVECTION-DOMINANT INDOOR FLOW FIELD

S. Murakami, D.Eng. *Member ASHRAE*
S. Kato, D.Eng. *Member ASHRAE*
S. Nagano
Y. Tanaka

ABSTRACT

Particle diffusion with gravitational sedimentation has been investigated. The property of particle diffusion becomes complicated with the increase of particle size because of the effect of gravitational sedimentation.

Maintaining a high degree of cleanliness in a clean room requires the ability to predict and control the diffusion characteristics of various sizes of airborne particles in the room. This study seeks to establish a method of predicting the diffusion characteristics of such airborne particles in a conventional flow-type clean room by numerical simulation based on the k-ϵ two-equation turbulence model and by the particle diffusion model considering gravitational sedimentation. In order to validate the accuracy of the simulations, the authors compared the numerical simulations with the experimental results. A good correspondence was found between the experiments and the numerical simulations of airflow fields.

Since it is rather difficult to examine the characteristics of the diffusion field of particle sizes larger than 10 μm by experimental methods, the technique of numerical simulation was used to systematically analyze the effect of particle size on the diffusion fields under the effect of gravitational sedimentation.

Diffusion fields with particle sizes smaller than 4.5 μm in diameter are regarded as having no gravitational sedimentation in a conventional flow-type clean room with a convection-dominant flow field. In cases of larger particle size, i.e., 50 or 100 μm, the effect of gravitational sedimentation must be taken into account.

INTRODUCTION

This study is one of a continuing series of efforts to predict and analyze the diffusion characteristics of airborne particles in clean rooms by means of experiments and numerical simulations. Predicting and controlling such diffusion characteristics are particularly important when designing clean rooms for high levels of cleanliness and maintaining their efficiency. Airborne particles are often assumed to be passive contaminants, that is, assumed to move in the same manner as the airflow under the prevailing influence of advection and diffusion. This assumption is adequate when predicting the diffusion characteristics of small-diameter airborne particles in clean rooms. However, particles with a certain scale of diameter have their own inherent properties of coagulation, sedimentation, and deposition that are different from those of gaseous contaminants, and it then becomes necessary to examine the inherent properties of advection and diffusion of such particles throughout the room by taking these factors into account.

Many previous studies have confirmed the effectiveness of analyzing diffusion fields in conventional flow-type clean rooms by numerical simulation. The authors and others have confirmed that numerical simulation based on the k-ϵ two-equation turbulence model reproduces the three-dimensional isothermal airflow fields of a clean room with sufficient accuracy (Murakami et al. 1987; Nielsen 1988; Baker et al. 1988). The authors have also confirmed through many studies that numerical simulation of gas diffusion where the gas has the same specific density as air will reproduce the results of model experiments concerned with contaminant distributions in a clean room (Murakami et al. 1988, 1989). However, for the diffusion of airborne particles as affected by gravitational sedimentation, there are few studies on particle concentration distribution over the whole room that consider the inherent properties of the airborne particles and gravitational sedimentation (Busnaina et al. 1988).

This study thus examines the validity of simulations of airborne particle behavior in clean rooms. There are many difficulties in carrying out accurate experiments that analyze the behavior of airborne particles with larger

Shuzo Murakami is a professor and **Shinsuke Kato** is an associate professor at the Institute of Industrial Science, University of Tokyo, Japan. **Shin-ichiro Nagano** and **Yukihiko Tanaka** are researchers at the Technical Research Institute, Fujita Corporation, Kanagawa-ken, Japan.

diameters. It is difficult to continuously generate airborne particles larger than 5 μm in diameter in an experiment. Also, in such experiments, particle loss often occurs as a result of adhesion to the sampling tubes used for measuring particle concentration. Consequently, it is difficult to examine, by model experiments, the effect of gravitational sedimentation of such large particles on the diffusion fields in the room. Therefore, the purpose of this study is to systematically analyze these effects by numerical simulation.

BASIC CONDITIONS FOR ANALYSIS

Size of Airborne Particles

Particles that are troublesome with regard to control of cleanliness in actual clean rooms are usually considered to be those about 0.3 to 4.5 μm in diameter. However, to clearly examine the effects of gravitational sedimentation on diffusion, the analysis given here includes particles up to 100 μm in diameter. A maximum concentration of about 10^8 particles/m^3 is assumed. The gravitational settling velocity is calculated considering the properties of monodispersed standard polystyrene globular particles (density = 1.05 g/cm^3).

Advection and Turbulent Diffusion of Airborne Particles

The relaxation time of airborne particles, τ, is extremely small, i.e., about 1×10^{-7} s for particles 0.1 μm in diameter at a density of 1 g/cm^3, about 3×10^{-6} s for particles 1 μm in diameter, and about 3×10^{-4} s for particles 10 μm in diameter. The diffusion coefficient given by Brownian motion is extremely small when compared to the 0.15 cm^2/s of kinematic viscosity of air, i.e., 8×10^{-6} cm^2/s for particles 0.1 μm in diameter, 3×10^{-7} cm^2/s for those 1 μm in diameter, and 2×10^{-8} cm^2/s for those 10 μm in diameter. For these reasons, the passive scalar contaminant is assumed to be such that, when considering advection and turbulent diffusion of a simple airborne substance of small diameter in a room, it moves in exactly the same way as airflow to a first approximation, without interfering with the movement of the airflow. However, in some cases it is necessary to take account of body forces, such as gravity, electrostatic forces, etc., if the particles are affected by their effects. Particular attention is paid to the effects of gravity. The gravitational settling velocity, τg (g = gravitational acceleration = 9.8 m/s^2), is often difficult to ignore with large particle sizes, so the usual hypothesis of passive scalar contaminants cannot be maintained (e.g., 0.003 m/s for particles 10 μm in diameter [see Table 1]).

Coagulation of Airborne Particles

The effect of coagulation depends largely on the initial particle concentration. If the initial value is about 10^8 particles/m^3, as assumed in this study, the change in particle concentration due to coagulation is found by the preliminary analysis to be extremely small, even when the influence of diffusion by Brownian motion is included. In the range of particle concentration considered in this study, it is thus reasonable to assume that the particle size distribution is not changed by coagulation. The synthesized diffusion properties of airborne particles with various particle sizes may possibly be evaluated using a simple superposition of the respective diffusion fields of each particle size.

Deposition of Airborne Particles

Generally speaking, the phenomenon of deposition becomes effective within a small-length scale related to Brownian diffusion or electrostatic force. Therefore, this effect becomes important when considering the behavior of airborne particles near a wall or equipment. However, when considering the diffusion characteristics of airborne particles in the room as a whole, the significance of changes in the particle concentration due to deposition may be considered negligible. In this study, the effect of deposition is therefore considered only where it results from gravitational sedimentation.

FULL-SCALE MODEL EXPERIMENTS

Figure 1 shows the configuration of the full-scale clean room used for measurements (L × W × H = 3,290 mm × 5,850 mm × 2,800 mm), and Table 2 gives the specifications of the clean rooms used for the simulations and experiments. The experiments and simulations

TABLE 1
Gravitational Settling Velocity by Particle Size

Particle size (μm)	0.31	1.0	4.5	10	50	100
Gravitational settling velocity (m/s)	4.5 x10^{-6}	3.5 x10^{-5}	6.2 x10^{-4}	3.0 x10^{-3}	7.5 x10^{-2}	3.0 x10^{-1}

NOTE: Particle density is assumed to be 1 g/cm^3 (polystyrene, etc.) and particles of globular shape. Calculated using Stokes' gravitational settling equation.

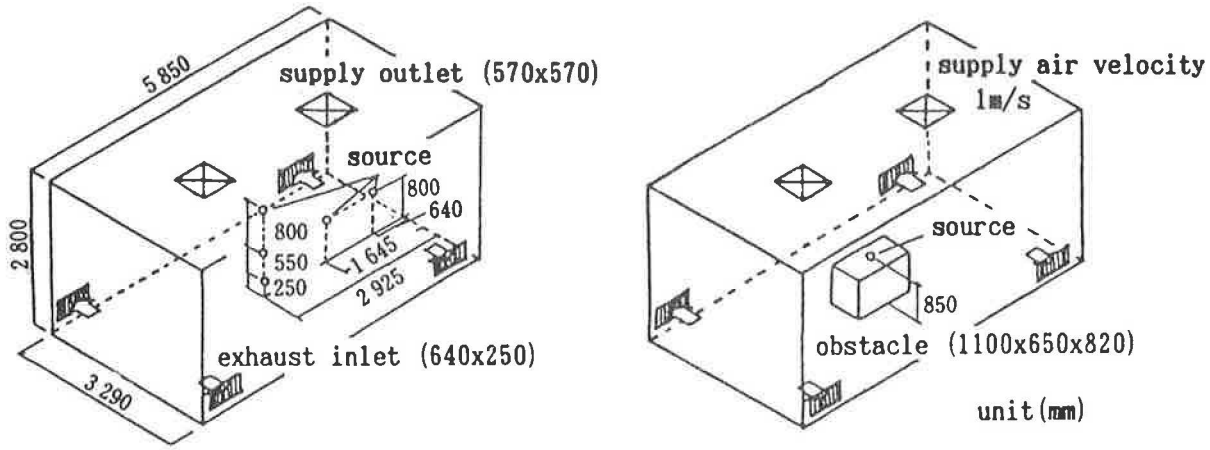

(a) Type 1 (no obstacle)

(b) Type 2 (with obstacle)

Figure 1 Model clean rooms used for full-scale experiments and simulations.

were carried out under conditions of an isothermal flow field (supply velocity = 1 m/s). The air exchange rate was 40 per hour in both Type 1 and Type 2 experiments (two supply outlets, four exhaust inlets). The model equipment is installed in the middle of the Type 2 room as an airflow obstacle (L × W × H = 1,100 mm × 650 mm × 820 mm).

Measurements of airflow fields were taken using thermistor anemometers reading the scalar velocity, and direction was determined by visual observations using a smoke tester. To measure the concentration of airborne particles, an optical particle counter was used. A sampling tube (6 mm in inside diameter, 5 m in length) with a pumping speed of 4.7×10^{-5} m^3/s (0.1 ft^3/min) and a measurement time of 60 seconds was also used. Particles were generated by an atomizer using two types of monodispersed polystyrene standard particles (average particle sizes of 0.31 and 1.0 μm, respectively, and a density of 1.05 g/cm^3 in common). Considering the particle concentration frequently observed in clean rooms, the generation of particles was set at about 10^5 particles/s (the nominal concentration in the room [particle generation rate divided by airflow rate] is about 3×10^5 particles/m^3), and the particle concentration at the source was about 6×10^8 particles/m^3.

As the particle concentration was rather high near the source, the degree of coagulation near the source had to be examined. The half-value period of particle number due to turbulence coagulation in the case of a monodispersed aerosol of 1.0 μm particle size (turbulence coagulation constant $K_T = 10^{-16}$ m^3/s with ϵ_o assumed to be 3.3×10^{-3} m^2/s^3) is about 10^7 seconds, according to preliminary calculations based on the simple coagulation model $dn/dt = -K_T n^2$ (Takahashi 1982). This value (10^7 seconds) is sufficiently large compared with the nominal diffusion time in a room of 180 seconds (the length of time required for one air exchange), so the influence of the turbulence coagulation can be ignored. The effect of coagulation due to the Brownian motion has already been shown to be much smaller.

NUMERICAL SIMULATION

The configurations and specifications of the model clean rooms used for simulation were the same as those shown in Figure 1 and Table 2, respectively. The isothermal three-dimensional airflow properties were analyzed on the basis of the k-ϵ model. Table 3 shows the basic equation and the numerical constants, while Table 4 gives the boundary conditions and finite-difference scheme. The

TABLE 2
Specifications of Model Clean Rooms Analyzed

Type of clean room	Number of supply outlets	Number of exhaust inlets	Supply outlet velocity (m/s)	Height of source (m)	Volume of air change (m^3/s)	Airflow obstacle
Type 1	2	4	1.0	0.25	0.64	No
Type 1	2	4	1.0	0.8	0.64	No
Type 1	2	4	1.0	1.6	0.64	No
Type 2	2	4	1.0	0.85	0.64	Yes

TABLE 3
k-ε Two-Equation Model (Three-Dimensional)

(1) Continuity equation

$$\frac{\partial U_i}{\partial X_i} = 0$$

(2) Momentum equations

$$\frac{\partial U_i}{\partial t} + \frac{\partial U_i U_j}{\partial X_j} = - \frac{\partial}{\partial X_i}\left(\frac{P}{\rho} + \frac{2}{3}k\right) + \frac{\partial}{\partial X_j}\left\{\nu_t \left(\frac{\partial U_i}{\partial X_j} + \frac{\partial U_j}{\partial X_i}\right)\right\}$$

(3) Transport equation for turbulent energy k

$$\frac{\partial k}{\partial t} + \frac{\partial k U_i}{\partial X_j} = \frac{\partial}{\partial X_j}\left(\frac{\nu_t}{\sigma_1}\frac{\partial k}{\partial X_j}\right) + \nu_t S' - \varepsilon$$

(4) Transport equation for turbulent energy dissipation ε

$$\frac{\partial \varepsilon}{\partial t} + \frac{\partial \varepsilon U_i}{\partial X_j} = \frac{\partial}{\partial X_j}\left(\frac{\nu_t}{\sigma_2}\frac{\partial \varepsilon}{\partial X_j}\right) + C_1\frac{\varepsilon}{k}\nu_t S' - C_2\frac{\varepsilon^2}{k}$$

(5) Expression of eddy kinematic viscosity based on eddy viscosity modelling

$$\nu_t = C\mu\frac{k^2}{\varepsilon} = C\mu\frac{k^{3/2}}{\ell}$$

(6) Transport equation for concentration C

$$\frac{\partial C}{\partial t} + \frac{\partial C U_j}{\partial X_j} + \frac{\partial C W_s}{\partial X_3} = \frac{\partial}{\partial X_j}\left(\frac{\nu_t}{\sigma_3}\frac{\partial C}{\partial X_j}\right) + C_s$$

Here, $S' = 2 S_{ij} S_{ij} = 2\left\{\frac{1}{2}\left(\frac{\partial U_i}{\partial X_j} + \frac{\partial U_j}{\partial X_i}\right)\right\}^2$

$\sigma_1=1.0, \sigma_2=1.3, \sigma_3=1.0, C\mu=0.09, C_1=1.44, C_2=1.92$

TABLE 4
Boundary Conditions and Finite-Difference Scheme for Numerical Simulation

(1)	Supply Outlet	$U_t=0.0$, $U_n=U_{out}$, $k_o=0.005\,(m^2/s^2)$, $\ell_o=0.285\,(m)$, $C=C_o$ subscript t, n: tangential and normal direction with respect to outlet surface. U_o: supply outlet velocity (=1.0 m/s) C_o: supply concentration (=0.0 kg/m³)
(2)	Exhaust Inlet	$U_t=0.0$, $U_n=U_{in}$, $\partial k/\partial n=0.0$, $\partial \varepsilon/\partial n=0.0$, $\partial C/\partial n=0.0$ U_{in}: exhaust inlet velocity (=1.0 m/s)
(3)	Wall Surface	$(\partial U_t/\partial n)_{n=0}=m(U_t)_{n=h}/h$, $U_n=0.0$, $\partial k/\partial n=0.0$, $\partial C/\partial n=0.0$, $(\varepsilon)_{n=h}=(C\mu\, k_{n=h}^{3/2})/(C\mu^{1/4}\kappa h)$ h: distance from wall surface to the center of the near-wall cell m: 1/7, power law profile $U_t \propto Z^m$ is assumed near the wall κ: 0.4, von Karman constant
(4)	Finite Difference Scheme	Space differential: 1) QUICK scheme : momentum equation 2) First-order upwind scheme : transport equations for k, ε and C 3) Centered differential scheme for all others Time differential: Adams-Bashforth scheme with second-order accuracy

NOTE: This simulation is performed using full-scale physical parameters.

analyses of the airflow and diffusion fields were performed with a mesh system of 43(X) × 20(Y) × 23(Z) in Type 1 and 43(X) × 20(Y) × 20(Z) in Type 2. Figure 2 shows the mesh system for Type 1.

In the numerical simulations of the diffusion of airborne particles, the following assumptions were applied on the basis of the previously described assumptions. When the gravitational settling velocity is assumed to be zero, contaminant diffusion is assumed to be the same as that of a completely passive scalar contaminant. That is, (1) distribution changes due to particle loss from coagulation and deposition are ignored, (2) gravitational sedimentation is ignored, and (3) airborne particles are considered as being transported as one body with the air. In all simulations, it is assumed that particle generation is constant, and the rate of generation is chosen so that nominal concentration (particle generation rate divided by airflow rate) is 1.0.

When gravitational settling velocity is considered, assumption 1 (neglecting the effects of coagulation and deposition by Brownian diffusion) is applied, but assumptions 2 and 3 are not because particles are deposited on the floor by gravity. The particle diffusion is assumed to follow Equation 6 in Table 3, and airborne particles on the floor and top surfaces of the obstacle are assumed to be removed from the air by sedimenting and accumulating

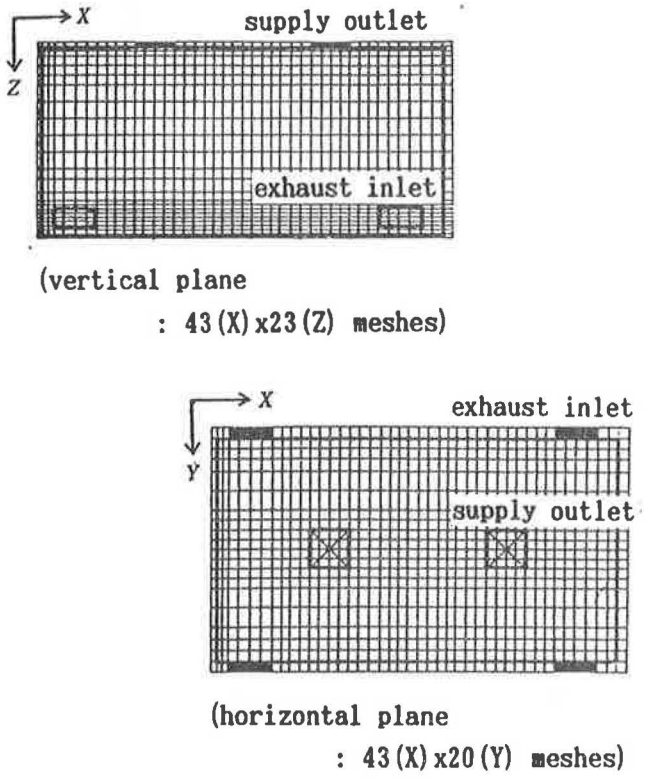

Figure 1 *Model clean rooms used for full-scale experiments and simulations.*

due to the downward concentration flux as a result of gravitational sedimentation.

The total concentration flux toward the floor, namely, the deposition rate onto the floor, is expressed as $(-U_3C - W_sC + \nu_t/\sigma_3 \cdot \partial C/\partial X_3)$. When considering the gravitational settling velocity in this simulation, the resulting concentration flux toward the floor is given as W_sC. It is calculated assuming a normal velocity, U_3, and a normal concentration gradient, $\partial C/\partial X_3$, at the floor surface as zero. Furthermore, the effect of deposition by Brownian motion onto the floor is ignored. The validity of the simulation results is examined by comparing them with the results of the full-scale experiment. In these experiments, where monodispersed polystyrene standard particles of 0.31 μm are used, gravitational sedimentation is found to be negligible.

COMPARISON OF EXPERIMENTS AND NUMERICAL SIMULATIONS WITHOUT GRAVITATIONAL SEDIMENTATION

Flow Fields in Type 1 Room Model

Figures 3a, 3c, and 3e show the results of simulations and Figures 3b, 3d, and 3f show the results of the full-scale experiments. Both indicate approximately symmetrical velocity fields, and the averaged flow fields correspond well with each other. The supply jet spreads in all directions after reaching the floor (Figures 3c, 3d) and rises along the walls (Figures 3a, 3b, 3e, 3f). Between the supply outlet jets, the airflows along the floor collide, forming a small rising stream (Figures 3a, 3b). In the cross section (Figures 3e, 3f), a recirculation consisting of a downward flow in the center and a rising flow at the walls appears due to the effects of the supply outlet jets. However, a distinct downward flow is observed in the center area in the case of the simulation, while in the experiments this airflow velocity is small and somewhat different from the simulation (Figures 3a, 3b, 3e, 3f). Although there are some unknowns, including the shortcomings of the k-ϵ model itself, one reason for this difference may be that the average velocity profile and the turbulent flow properties at the supply outlet cannot be precisely matched for the simulations and the experiments. This difference between simulated and measured airflows causes a small lack of correlation between the diffusion characteristics of the simulations and the experiments when the height of the source is changed, as will be described below.

Diffusion Fields of Type 1 Room Model

The diffusion properties of monodispersed airborne particles 0.31 μm in diameter, as measured in experiments, are shown in Figures 4, 5, and 6. Since the gravitational settling velocity of 0.31-μm particles is 4.5×10^{-6} m/s, the effect of gravitational sedimentation on diffusion properties is small, as is experimentally examined in the appendix. The space concentration distribution is presented as the dimensionless concentration divided by the average concentration at the exhaust (nominal diffusion concentration) in both experiments and simulations. Except in the cases shown in Figures 4 and 5, the diffusion properties are almost symmetrical, so only one-half of the distribution is shown.

Case of Airborne Particles Generated Near Wall (Figure 4)

Although there are some differences in the distribution of high-concentration areas, the clean domain (with a dimensionless concentration of less than 0.4) is very similar in the simulation (Figure 4a) and in the experiment (Figure 4b).

Case of Airborne Particles Generated Under Supply Jet (Figure 5)

Except for small differences in the shape of the dimensionless concentration contour line, the pattern of concentration distributions is almost the same in the simulation (Figure 5a) and in the experiment (Figure 5b).

Case of Source Height Being Different (Figure 6)

The diffusion patterns in the cases of source heights being 0.25 and 0.8 m (Figures 6a, 6b, 6c, 6d) show good

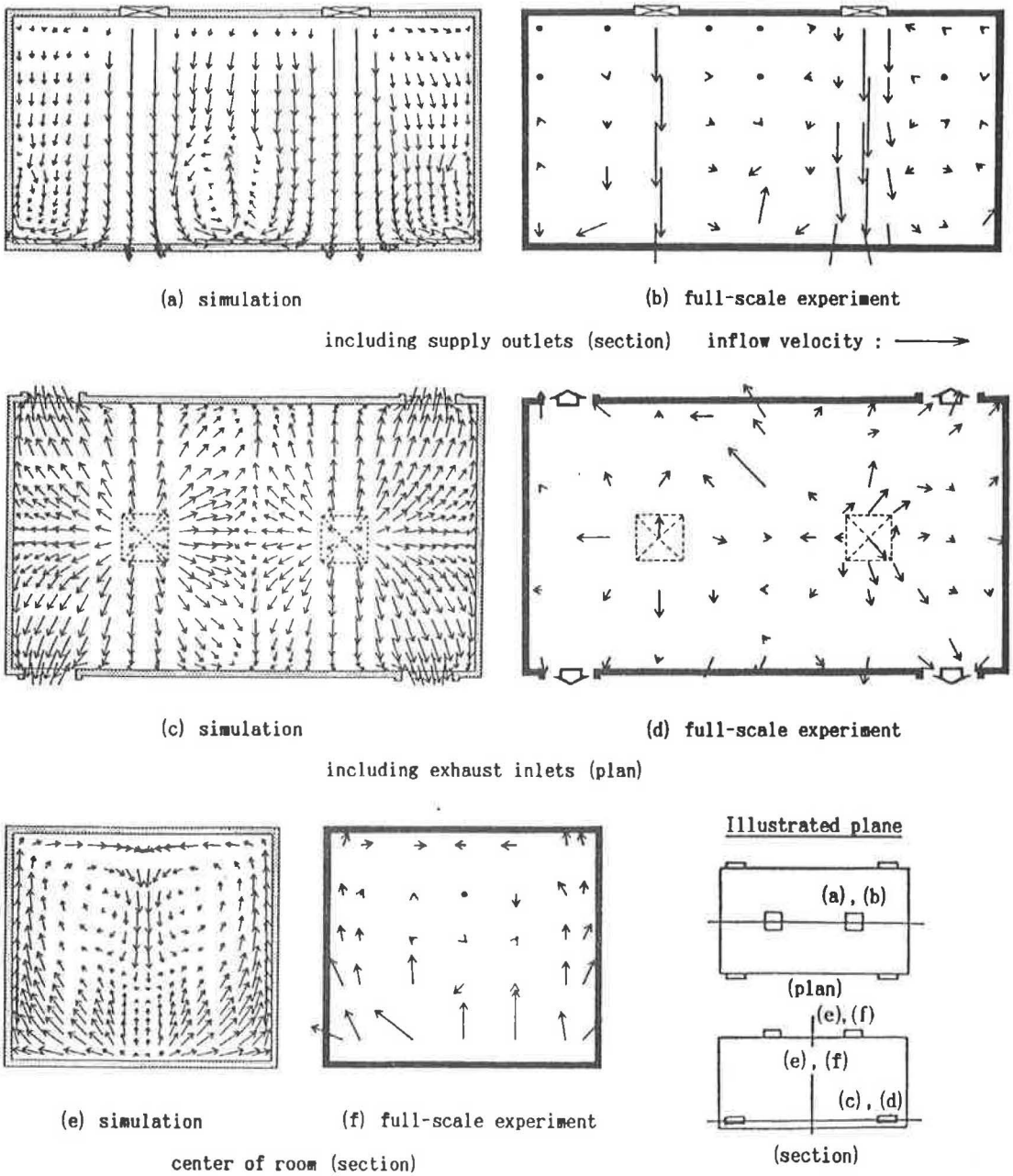

Figure 3 *Comparisons of flow fields of Type 1 room model (with obstacle).*

correspondence between the simulations and the experiments. When the source height is 1.6 m (Figures 6e, 6f), the domain of dimensionless concentration above 1.6 is larger in the simulation than in the experiments. This is because at the source height 1.6 m, airflow conditions differ slightly between the simulation and experiments, as stated before.

Airflow Fields in Type 2 Room Model

Figures 7a and 7b show the results of simulations and experiments when an obstacle is placed in the center of the room. The airflow fields of the simulation (Figure 7a) and the experiment (Figure 7b) correspond approximately, such as where the supply jet impinges on the floor and diffuses in all directions, becoming a rising airflow along the side of the obstacle and the wall of the room.

Diffusion Fields in Type 2 Room Model

When the source is located in an area of weak airflow on the upper surface of the obstacle, the airborne particles stagnate, causing a high concentration domain. Thus, the results of the simulation (Figure 8a) and the experiment (Figure 8b) match well. This can be expected, since the airflows in the numerical simulations and the experiments also correspond closely (Figure 7).

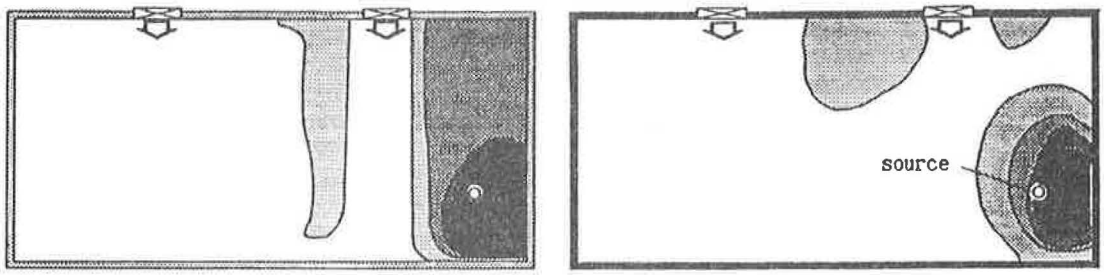

(a) simulation
(zero gravitational settling velocity)

(b) full-scale experiment
(particle size 0.31 μm)

including supply outlets (section)

Figure 4 *Comparison of contaminant distributions of Type 1 room model (no obstacle, source located near the wall).*

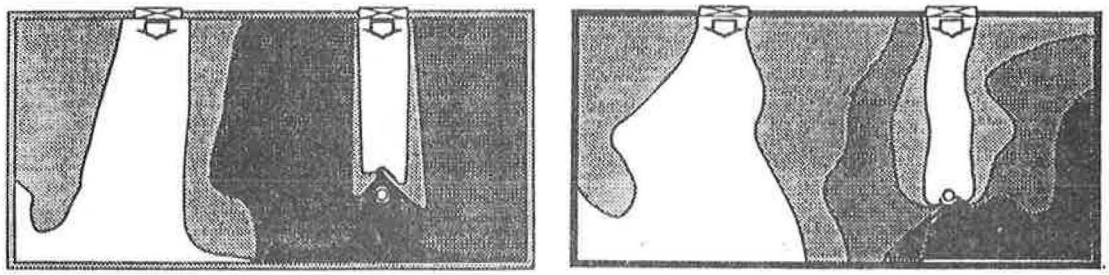

(a) simulation
(zero gravitational settling velocity)

(b) full-scale experiment
(particle size 0.31 μm)

including supply outlets (section)

Figure 5 *Comparison of contaminant distributions of Type 1 room model (no obstacle, source located just under supply jet).*

Discussion of Negligible Gravitational Sedimentation

As is experimentally shown in the appendix, airborne particles of about 0.3 μm in diameter have approximately the same diffusion properties as a gas of the same density as air, as far as the time-averaged space concentration distribution is concerned. This is due to the fact that the characteristic time scale of diffusion in areas where advection and turbulent diffusion are predominant is small compared with the characteristic time scale related to inherent particle properties such as gravitational sedimentation. Thus, the spatial concentration distribution of particles about 0.31 μm in diameter, for which gravitational sedimentation can be ignored, is well predicted by the simulation with no consideration of sedimentation, as would be expected, since previous studies (Murakami et al. 1987, 1988) confirmed that the diffusion properties of a gas equal in density to air can be well reproduced by simulation.

NUMERICAL ANALYSIS CONCERNING EFFECT OF GRAVITATIONAL SEDIMENTATION

The diffusion properties of airborne particles are examined in the case of gravitational sedimentation for Type 1 and Type 2 airflow fields. For comparison, the results of zero gravitational settling velocity are also shown.

Diffusion Fields for Type 1 Room Model (Figure 9a)

Figure 9a shows the diffusion properties of monodispersed polystyrene standard particles of 0.31-μm diameter as measured by full-scale experiments. Only one-half of the symmetrical results are shown. Table 5 shows the average concentration in the room and at the exhaust inlet for each particle size.

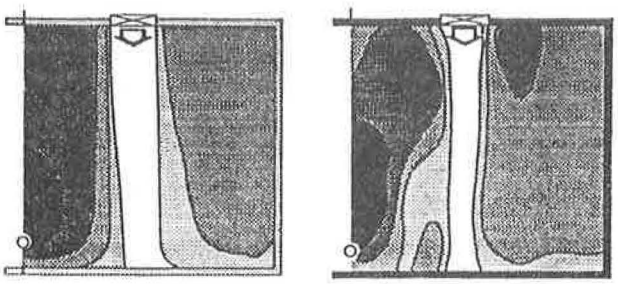

(a) simulation (b) full-scale experiment

height of source is 0.25 m

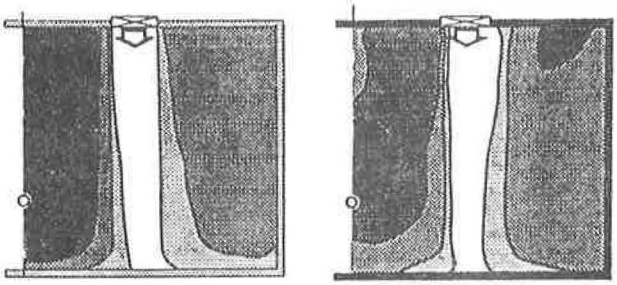

(c) simulation (d) full-scale experiment

height of source is 0.8 m

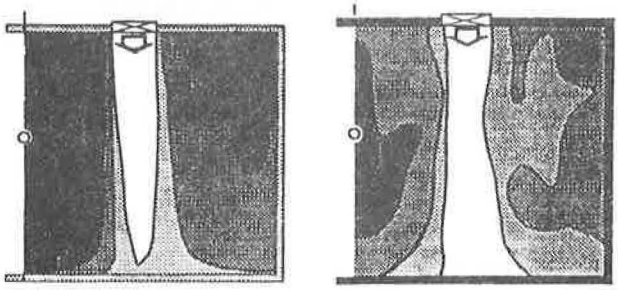

(e) simulation (f) full-scale experiment

height of source is 1.6 m

Dimensionless concentration

Figure 6 *Comparison of contaminant distributions of Type 1 room model (no obstacle, height of sources is changed, simulation: gravitational settling velocity is assumed to be 0; experiment: particle size = 0.31 μm).*

Case of Zero Gravitational Settling Velocity (Figure 9b)

As was stated above, the results of the simulations correspond well with those of the experiments.

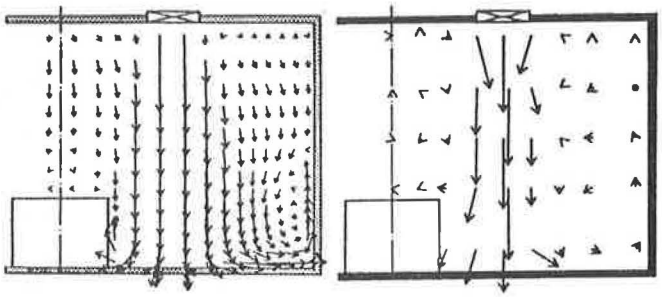

(a) simulation (b) full-scale experiment

including supply outlets (section) inflow velocity :⟶

Figure 7 *Comparison of flow fields of Type 2 room model (with obstacle).*

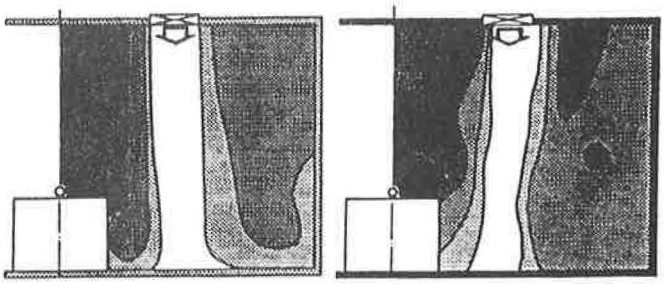

(a) simulation (b) full-scale experiment

(zero gravitational settling velocity) (particle size 0.31 μm)

including supply outlets (section)

Dimensionless concentration

Figure 8 *Comparison of contaminant distributions of Type 2 room model (with obstacle).*

Cases with Various Gravitational Settling Velocities Considered by Particle Size (Figures 9c through 9h)

The results of the simulations for particle sizes of 0.31 to 10 μm (Figures 9c through 9f) do not differ significantly from those with zero gravitational settling velocity. However, the larger the particle size, i.e., 50 and 100 μm (Figures 9g, 9h), the smaller the diffusion area of the airborne particles. When the clean domain with a dimensionless concentration below 0.4 extends over a greater portion of the room, the results of the simulations are very different from those of the experiments with a particle size of 0.31 μm. As shown in Table 5, the room-average concentration is about 1.7 when the

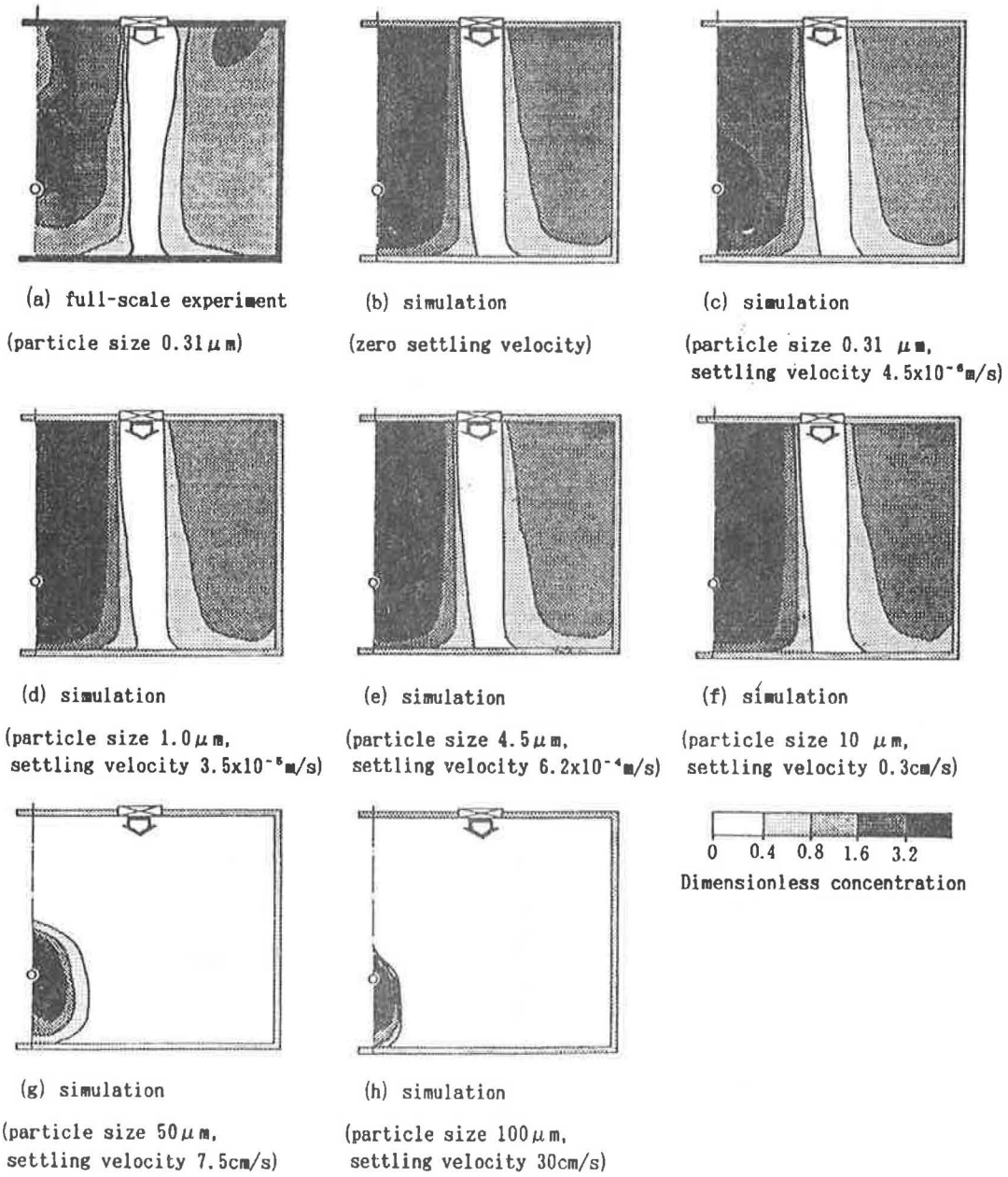

Figure 9 *Comparisons of contaminant distributions of Type 1 room model (no obstacle, gravitational settling velocity is considered).*

TABLE 5
Average Concentration in Room and at Exhaust Inlet by Particle Size

Type of clean room	Airflow obstacle	Average concentration	Particle size (μm)					
			0.31	1.0	4.5	10	50	100
Type 1	No	Room	1.70	1.70	1.68	1.59	0.52	0.11
		Exhaust	0.99	0.99	0.98	0.91	0.11	0.00
Type 2	Yes	Room	1.84	1.84	1.77	1.47	0.05	0.01
		Exhaust	0.99	0.99	0.95	0.77	0.01	0.00

NOTE: Value of concentration is normalized with that at the exhaust in the case of 0.31 μm particles.

particle size is below 4.5 μm, while it is about 0.5 when the particle size is 50 μm, showing a distinct difference in the effect of deposition between the two cases. The average concentration at the exhaust inlet decreases as the particle size increases, directly reflecting the result of deposition on the floor. In particular, the concentration at the exhaust inlet falls to zero in the case of 100-μm particles; consequently, it may be concluded that most particles accumulate and deposit on the floor without being exhausted from the room. The experiments described in the appendix also show that the effects of gravitational sedimentation on the diffusion of 4.5-μm particles are very small, confirming the findings observed in the simulation results.

Diffusion Fields for Type 2 Room Model (Figure 10a)

Particles are assumed to be generated in the calm region above the top surface of the obstacle.

Case of Zero Gravitational Settling Velocity (Figure 10b)

As already described, the simulation results well reproduce those of the experiments.

Cases with Various Gravitational Settling Velocities Considered by Particle Size (Figures 10c through 10h)

When particles are smaller than 4.5 μm (Figures 10c through 10e), the results from the simulation do not differ

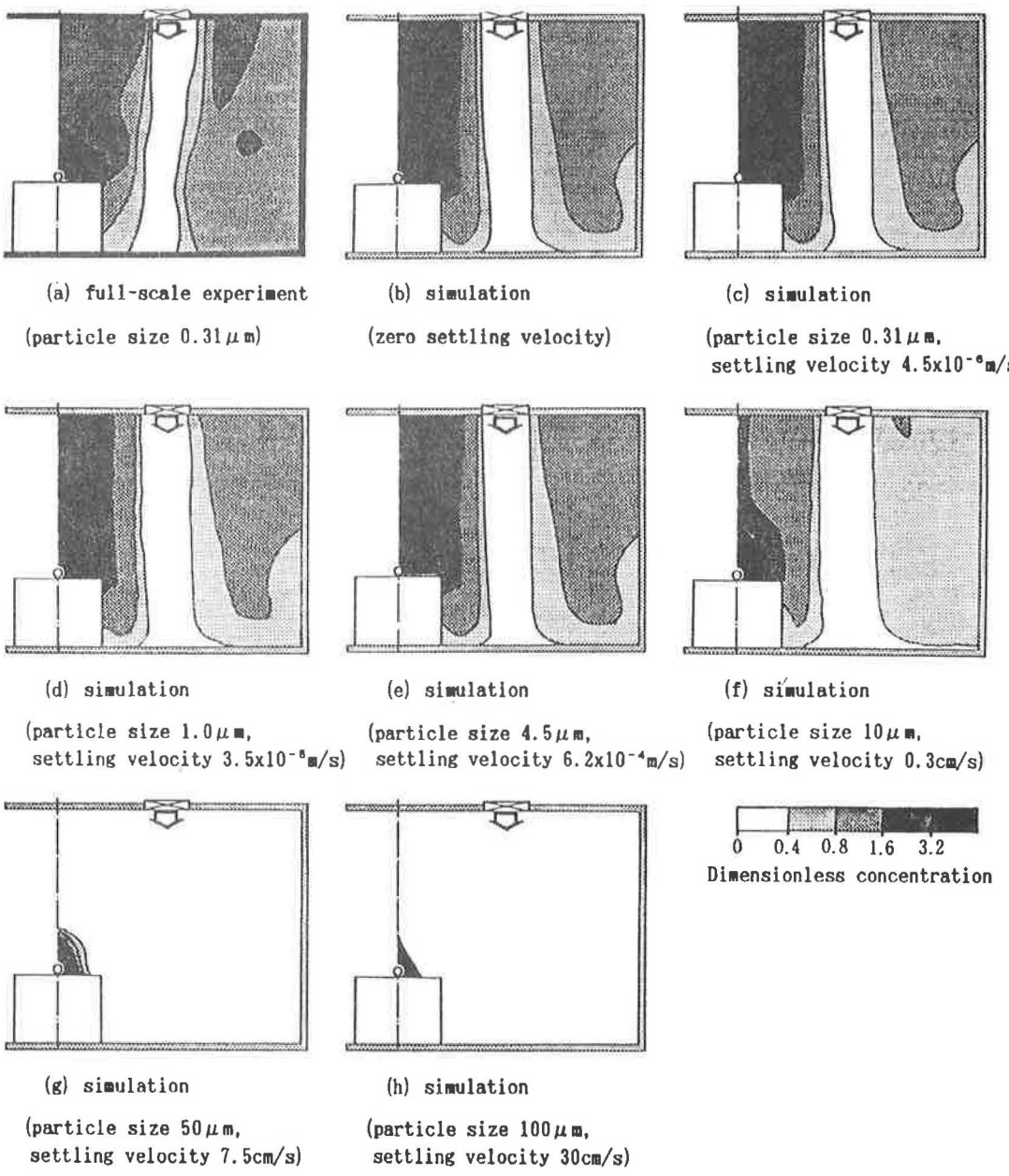

Figure 10 *Comparisons of contaminant distributions of Type 2 room model (with obstacle, gravitational settling velocity is considered).*

from those with zero gravitational settling velocity. When the particles are larger—10 μm (Figure 10f)—the influence of gravitational sedimentation begins to appear. As the particle size becomes even larger, 50 and 100 μm (Figures 10g, 10h), the diffusion of airborne particles becomes very small and the clean domain with a dimensionless concentration of less than 0.4 occupies the whole room. As shown in Table 5, the average concentration at the exhaust inlet is almost zero when the particle size is 50 μm, which is still smaller than the value of 0.11 given in the case of Type 1. This is the direct effect of deposition on the top surface of the obstacle, because deposition due to gravitational sedimentation is particularly effective when the vertical distance between the source and surface of the obstacle is small.

Discussion on the Effects of Gravitational Sedimentation

In this study, the characteristic time scale for turbulent diffusion and advection due to airflows in the room is estimated to be about 100 seconds on the basis of the air change rate in the room (40 per hour). On the other hand, in the case of Type 1, the time scale calculated by gravitational settling velocity (0.3 cm/s) for particles 10 μm in diameter is about 300 seconds from the source to the floor (0.8 m), or three times the characteristic time scale for turbulent diffusion due to the airflow in the room. However, the characteristic time scales calculated by gravitational settling velocity for particles 50 μm and 100 μm in diameter are very much shorter than for turbulent diffusion, about 10 seconds and 3 seconds, respectively. The difference in the ratio between the two characteristic time scales is well reflected in the concentration distributions, as shown in Figures 9 and 10. In other words, the effect of gravitational sedimentation can be predicted easily by the rough estimations of the two characteristic time scales related to sedimentation and turbulent diffusion. The effect of gravitational sedimentation becomes significant only when the former time scale falls to the same order as or to an order below the latter time scale.

CONCLUSIONS

As a method for predicting airborne particles in a conventional flow-type clean room, the numerical simulation method using the k-ϵ model and the particle diffusion model considering the effects of gravitational sedimentation were examined. The following results were obtained:

1. With regard to the concentration distribution of small airborne particles with negligible gravitational sedimentation, the experimental results are well reproduced by the simulation by means of the k-ϵ model, assuming a complete passive scalar contaminant.
2. In the diffusion fields examined here, airborne particles smaller than 4.5 μm show diffusion properties similar to those in the case of zero gravitational settling velocity. When the particles are larger, 50 or 100 μm, almost no diffusion takes place in the room; instead, particles accumulate on the floor. Consequently, the room takes on an entirely different concentration distribution. When the particle size is 10 μm, although the effects of gravitational sedimentation start to appear, diffusion properties similar to those of the 4.5-μm particles are observed.
3. A good indicator of the characteristic time scale for turbulent diffusion fields in the room is the air exchange rate. When the sedimentation time scale of airborne particles (calculated by the vertical distance from the source to the solid surface boundary and the gravitational settling velocity) is larger than or on the same order as this characteristic diffusion time scale, the diffusion fields do not differ much from that in the case of zero gravitational settling velocity. However, as the sedimentation time scale becomes smaller, the effects of gravitational sedimentation appear and the diffusion properties of airborne particles vary greatly from the case of zero gravitational sedimentation.

NOMENCLATURE

C_μ, C_1, and C_2	=	empirical constants in the turbulence model (see Table 3)
C	=	mean concentration of airborne particles
C_s	=	source term of airborne particles
C_r	=	correction term due to coagulation
D_T	=	eddy diffusivity coefficient
g	=	gravitational acceleration
k	=	turbulence energy
k_{out}	=	boundary value for k of inflow
K_T	=	turbulent coagulation constant
ℓ	=	length scale of turbulence
ℓ_{out}	=	boundary value for ℓ of inflow
L_o	=	representative length scale defined by width of supply outlet
P	=	mean pressure
Re	=	Reynolds number
W_S	=	settling velocity of airborne particles
U_i, U_j	=	components of velocity vector
U_o	=	representative velocity defined by inflow air velocity
ϵ, ϵ_o	=	turbulent energy dissipation
κ	=	von Karman constant, 0.4
ρ	=	density
ν_t	=	eddy kinematic viscosity
σ_1, σ_2, and σ_3	=	turbulence Prandtl/Schmidt number of k, ϵ, C (see Table 3)
τ	=	relaxation time of airborne particles

REFERENCES

Baker, A.J., R.M. Kelso, W.P. Noronha, and J.B. Woods. 1988. On the maturing of computational fluid dynamics in design of room air ventilation systems. *Building Systems: Room Air and Air Contaminant Distribution*, L.L. Christianson, ed., pp. 149-152. Atlanta: American Society of Heating, Refrigerating and Air-Conditioning Engineers, Inc.

Busnaina, A.A., S. Abuzeid, and M.A.R. Sharif. 1988. Three-dimensional numerical simulation of fluid flow and particle transport in a clean room. *Proceedings —Ins. of Environmental Sciences*: 326-330.

Murakami, S., and H. Komine. 1980. Measurement of three components of turbulent flow with tandem hot-wire probe. *Transactions of Architectural Institute of Japan* 297: 59-69.

Murakami, S., S. Kato, and Y. Suyama. 1987. Three-dimensional numerical simulation of turbulent airflow in ventilated room by means of a two-equation model. *ASHRAE Transactions* 93 (2): 621-642.

Murakami, S., S. Kato, and Y. Suyama. 1988. Numerical and experimental study on turbulent diffusion fields in conventional flow-type clean rooms. *ASHRAE Transactions* 94(2): 469-493.

Murakami, S., S. Kato, and Y. Suyama. 1989. Numerical study on diffusion field as affected by arrangement of supply and exhaust openings in conventional flow-type clean room. *ASHRAE Transactions* 95(2).

Nielsen, P.V. 1988. Numerical prediction of air distribution in rooms—Status and potentials. *Building Systems: Room Air and Air Contaminant Distribution*, L.L. Christianson, ed., pp. 31-38. Atlanta: American Society of Heating, Refrigerating, and Air-Conditioning Engineers, Inc.

Takahashi, M. 1982. *Fundamentals of aerosol science.* Tokyo: Yokendo Press.

BIBLIOGRAPHY

Chaturvedi, S.K., and T.O. Mohieldin. 1988. A CFD analysis of effects of vent location on pollutant concentration in rooms. *Building Systems: Room Air and Air Contaminant Distribution*, L.L. Christianson, ed., pp. 127-130. Atlanta: American Society of Heating, Refrigerating, and Air-Conditioning Engineers, Inc.

Choi, H.L., and L.D. Albright. 1988. Modeling effects of obstructions in slot-ventilated enclosures. *Building Systems: Room Air and Air Contaminant Distribution*, L.L. Christianson, ed., pp. 127-130. Atlanta: American Society of Heating, Refrigerating, and Air-Conditioning Engineers, Inc.

Janssen, J., and K. Krause. 1988. Numerical simulation of airflow in mechanically ventilated animal houses. *Building Systems: Room Air and Air Contaminant Distribution*, L.L. Christianson, ed., pp. 131-135. Atlanta: American Society of Heating, Refrigerating, and Air-Conditioning Engineers, Inc.

Kurabuchi, T., Y. Sakamoto, and M. Kaizuka. 1988. Numerical prediction of indoor airflows by means of the k-ϵ turbulence model. *Building Systems: Room Air and Air Contaminant Distribution*, L.L. Christianson, ed., pp. 57-67. Atlanta: American Society of Heating, Refrigerating, and Air-Conditioning Engineers, Inc.

APPENDIX

MODEL EXPERIMENTS ON EFFECTS OF GRAVITATIONAL SEDIMENTATION OF AIRBORNE PARTICLES

To examine in detail the effects of gravitational sedimentation on the diffusion properties of airborne particles, diffusion experiments in which the relative settling velocity of particles (the ratio of gravitational settling velocity to supply outlet velocity, W_S/U_o) is varied were performed using a one-fifth scale model room. The concentration distribution properties were measured in detail.

MODEL EXPERIMENT

Figure 11 shows the model used for the measurements (L × W × H = 1,050 mm × 770 mm × 490 mm). Table 6 shows the measurements for the experiments performed. The experiments were carried out using an isothermal supply jet. Contaminant sources were located at two points, one at a height of 35 mm (ⓐ point) and one at 245 mm (ⓑ point) in the center of the model room. The center section of the model room, including a supply outlet and an exhaust inlet, was measured. Airflow was measured in components in three directions using a hot-wire, tandem-type probe (Murakami et al. 1980).

To measure the concentration of airborne particles, the particle counter mentioned in the main text was used.

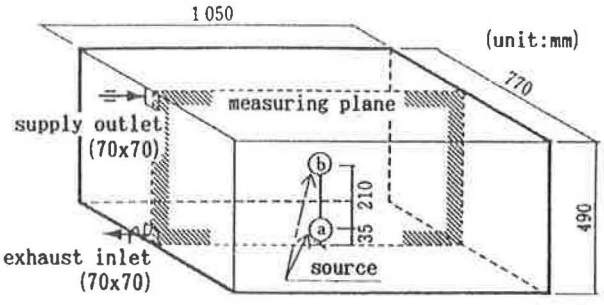

Figure 11 Room model and measuring plane (room model: one supply outlet and one exhaust inlet, one-fifth scale model).

TABLE 6
Classification of Measurements
(Change in Supply Outlet Velocity and Gravitational Settling Velocity)

Case No.	Measurement No.	Supply outlet velocity	Source position	Contaminant	Gravitational settling velocity (m/s)	W_s/U_o
	1			Ethylene	—	—
1	2		ⓐ	0.31 μm particle	4.5×10^{-6}	2.3×10^{-6}
	3	2.0 (m/s)		1.0 μm particle	3.5×10^{-5}	1.8×10^{-5}
	4			4.5 μm particle	6.2×10^{-4}	3.1×10^{-4}
	5	(Re=		Ethylene	—	—
2	6	9300)	ⓑ	0.31 μm particle	4.5×10^{-6}	2.3×10^{-6}
	7			1.0 μm particle	3.5×10^{-5}	1.8×10^{-5}
	8			4.5 μm particle	6.2×10^{-4}	3.1×10^{-4}
	9			Ethylene	—	—
3	10		ⓐ	0.31 μm particle	4.5×10^{-6}	9.0×10^{-6}
	11	0.5 (m/s)		1.0 μm particle	3.5×10^{-5}	7.0×10^{-5}
	12			4.5 μm particle	6.2×10^{-4}	1.2×10^{-3}
	13	(Re=		Ethylene	—	—
4	14	2300)	ⓑ	0.31 μm particle	4.5×10^{-6}	9.0×10^{-6}
	15			1.0 μm particle	3.5×10^{-5}	7.0×10^{-5}
	16			4.5 μm particle	6.2×10^{-4}	1.2×10^{-3}

Airborne particles were generated by spray drying, using an atomizer. Three types of monodispersed polystyrene standard particles (0.31, 1.0, and 4.5 μm in particle size and 1.05 g/cm^3 in density) were used. These particle sizes were chosen because the airborne particles that create various problems in clean rooms are usually up to 5 μm in diameter. The particle concentration just after the source was 10^8 to 10^{10} particles/m^3. With a sponge ball 4 cm in diameter stationed at the edge of the particle-generation tube, contaminants were uniformly generated in all directions with a discharge velocity of less than 1 cm/s, which has no effect on the airflow in the room. Since air is cooled in the atomization process, particular care was paid at this point to keep temperature differences in the model room within a tolerance of 0.1°C. To compare the diffusion properties of airborne particles, a diffusion experiment using a tracer gas of ethylene (one with the negligible buoyancy effect, specific gravity 0.97) was performed as well. To measure the tracer concentration, a flame ionization detector (gas chromatography) was used. The airflow and the concentration of airborne particles and contaminants are given here as average values over a measured time of 30 seconds.

DIMENSIONLESS DIFFUSION PARAMETER

The diffusion equation for airborne particles is

$$\frac{\partial C}{\partial t}+\frac{\partial CU_j}{\partial X_j}+\frac{\partial CW_3}{\partial X_3}=\frac{\partial}{\partial X_j}\left(D_T\frac{\partial C}{\partial X_j}\right)+C_r$$

where

C = particle concentration
D_T = eddy diffusivity coefficient
C_r = correction term due to coagulation, etc., which is ignored in the study
suffix 3 = component in vertical direction.

By making the equation dimensionless using the representative length scale, L_o, and the representative velocity scale, U_o, the following two parameters can be obtained:

$$\frac{U_o L_o}{D_T}$$ (turbulent Peclet number)

$$\frac{W_s}{U_o}$$ (settling velocity ratio).

In diffusion experiments using airborne particles, it is necessary to take care with these parameters. In this case, L_o and U_o (= 0.5 and 2 m/s) in each experiment are fixed and the effect of a change in W_S/U_o on the concentration distribution is examined in the model room under conditions of approximately the same Peclet number. Since D_T is proportional to L_o and U_o, the Peclet number becomes the same automatically.

RESULTS OF EXPERIMENTS

Airflow Properties in Model Room (Figure 12)

For both U_o = 2 m/s and U_o = 0.5 m/s, the airflow distribution is similar. The supply jet attacks the opposite

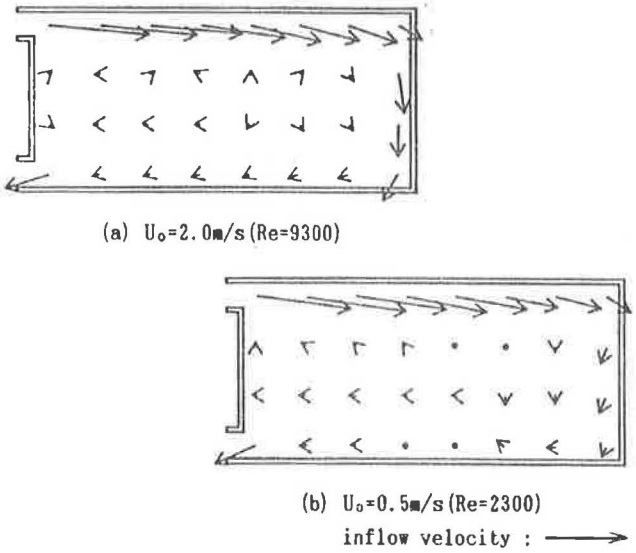

Figure 12 Measurement of flow fields by hot-wire, tandem-type probe.

wall and descends to the floor along the wall, from which it moves toward the exhaust inlet along the floor. Other areas have low airflow velocities. The descending flow near the surface of the wall on the right side of the room is slightly weaker when the result of U_o = 0.5 m/s compared with that of U_o = 2 m/s.

Diffusion Properties of Airborne Particles

Case 1 (U_o = 2 m/s, Source Point ⓐ, Figures 13a through 13d) The air in the supply jet is clean, and the concentration rises between the source and the exhaust inlet. No significant difference can be discerned between the concentration distribution of ethylene and the other three particle sizes. The characteristic velocity of advection and turbulent diffusion fields is defined as follows: characteristic length scale/characteristic time. This value is about 0.03 m/s assuming the characteristic time scale of the room as a whole to be on the order of 100 seconds (the reciprocal of the ventilation rate in the case of U_o = 0.5 to 2 m/s) and the characteristic length scale of the room as a whole to be 2.5 m (the distance along the streamline from the supply outlet to the exhaust inlet). The characteristic velocity scale, 0.03 m/s, is large compared to the gravitational settling velocity, 6.2 × 10^{-4} m/s, of particles 4.5 μm in diameter.

Case 2 (U_o = 2 m/s, Source Point ⓑ, Figures 14a through 14d) The air in the supply jet stays clean with a higher concentration only very near the source. No significant difference can be discerned between the concentration distributions of ethylene and the other three particle sizes.

Case 3 (U_o = 0.5 m/s, Source Point ⓑ, Figures 15a through 15d) The concentration distribution is similar to case 1. No significant differences can be discerned between the concentration distributions of ethylene and the other three particle sizes.

Case 4 (U_o = 0.5 m/s, Source Point ⓑ, Figures 16a through 16d) The clean domain resulting from the supply jet does not reach as far as the opposite wall. The concentration is higher as a whole compared to case 2. Figure 17 shows the correlation of concentration at each measuring point for No. 13 (ethylene) and No. 16 (particle size 4.5 μm). No significant difference can be seen between the concentration distributions of ethylene and the

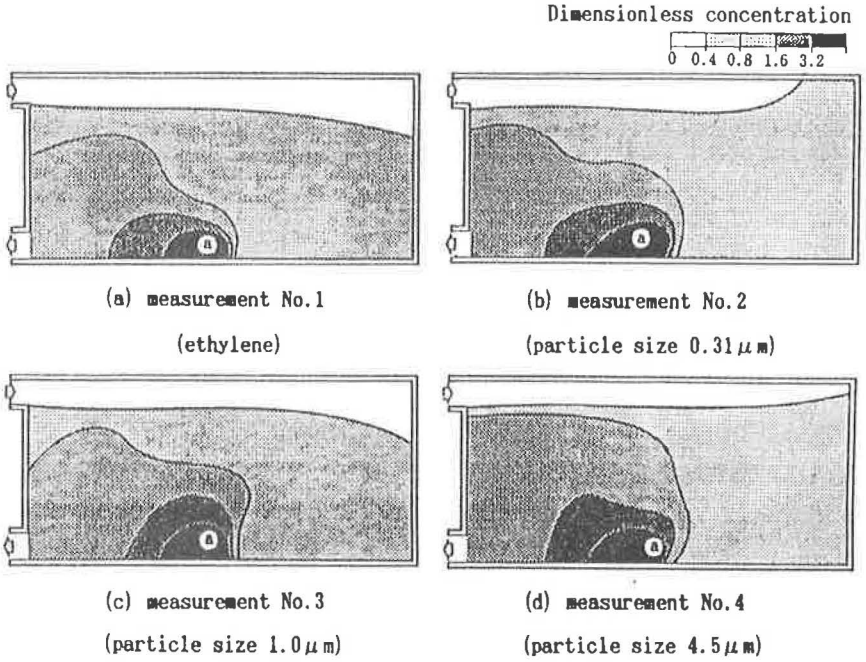

Figure 13 Comparisons of contaminant distributions in case 1 (U_o = 2 m/s).

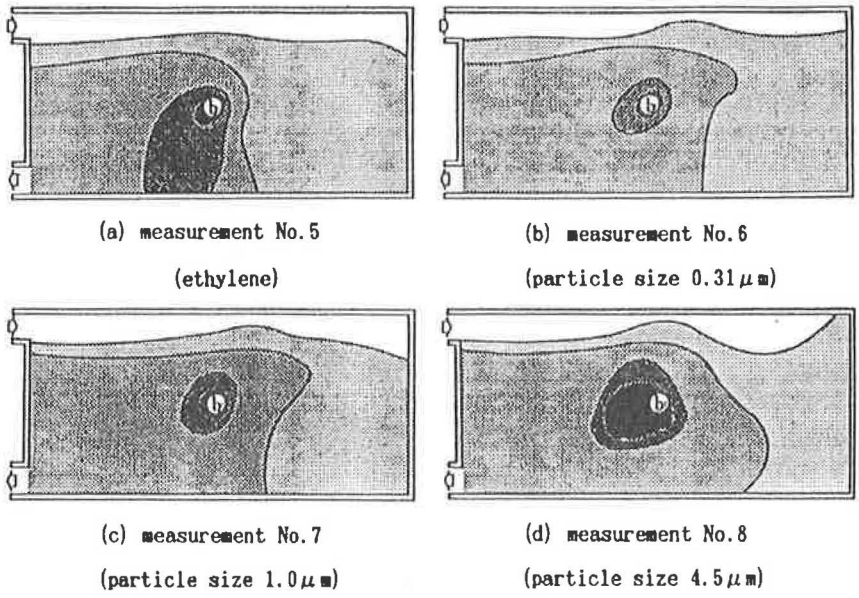

Figure 14 Comparisons of contaminant distributions in case 2 (U_o = 2 m/s).

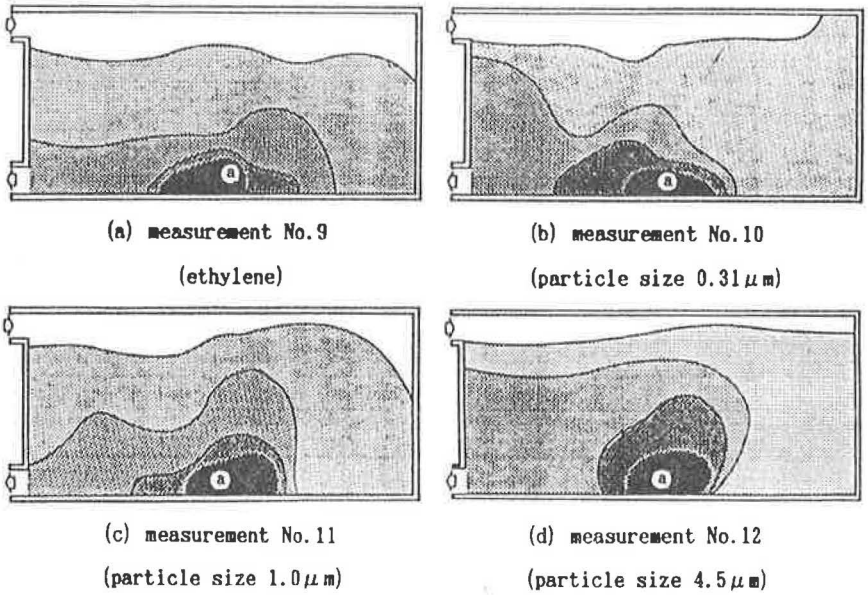

Figure 15 Comparisons of contaminant distributions in case 3 (U_o = 0.5 m/s).

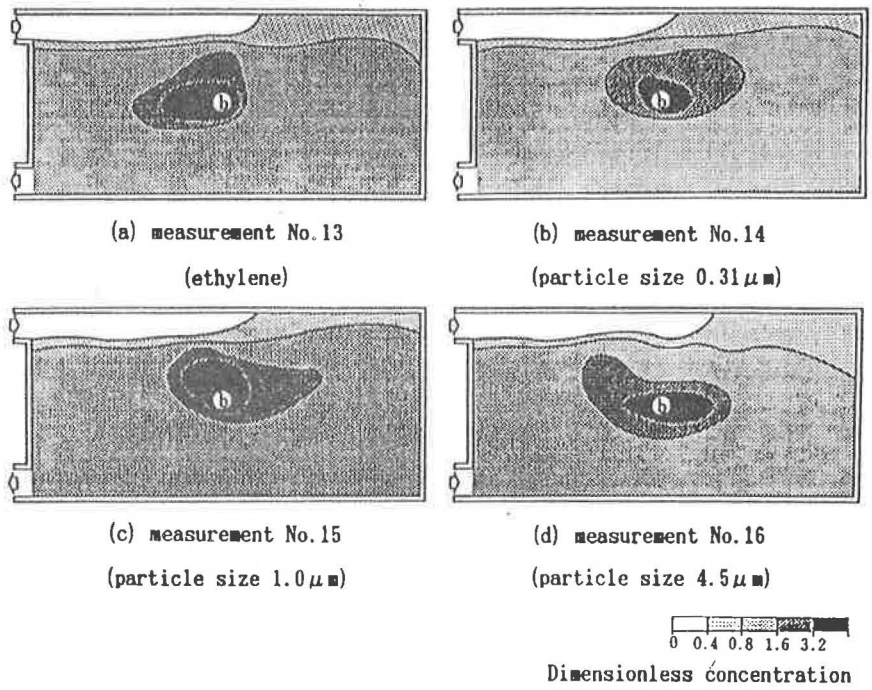

Figure 16 Comparisons of contaminant distributions in case 4 (U_o = 0.5 m/s).

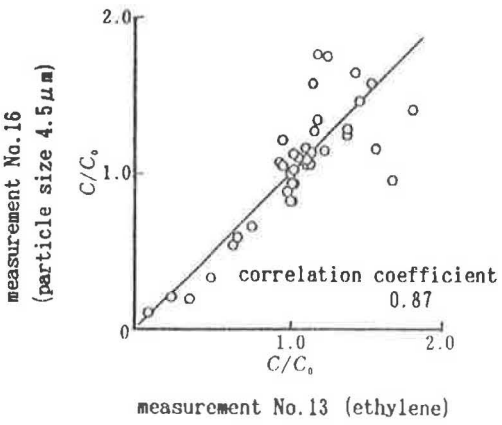

Figure 17 Correlation of C/C_0 between measurement No. 13 (ethylene) and No. 16 (particle size 4.5 μm).

4.5-μm-diameter particles. The correlation coefficient between the two is 0.87 and is sufficiently high.

CONCLUSIONS

1. The concentration distributions in diffusion experiments in which the ratio of the gravitational settling velocity of the airborne particles to the supply airflow velocity, W_S/U_o, is varied from 2.3×10^{-6} to 1.2×10^{-3} do not differ from those in the case of passive scalar contaminants.
2. Since the supply airflow velocity of an ordinary clean room is approximately 1 m/s, it may be concluded that the effects of gravitational sedimentation on the diffusion in a room can be practically ignored when the particles are smaller than about 5 μm in diameter.